

NUMERICAL AND EXPERIMENTAL STUDY ON METHANE HYDRATE PRODUCTION CHARACTERISTICS DURING DEPRESSURIZATION

Pengfei Wang^{1,2#}, Ying Teng^{3,4#}, Ruifang Huang¹, Yusheng Zhao^{1*}, Shenglong Wang^{5*}, Yongchen Song⁶

1 SUSTech Academy for Advanced Interdisciplinary Studies, Southern University of Science and Technology, Shenzhen 518055, China

2 School of Earth and Space Sciences, University of Science and Technology of China, Hefei 230026, China

3 Institute for Advanced Study, Shenzhen University, Shenzhen, 518060, China

4 College of Physics and Optoelectronic Engineering, Shenzhen University, Shenzhen 518060, China

5 Key Laboratory of Heat Transfer Enhancement and Energy Conservation of Education Ministry, School of Chemistry and Chemical Engineering, South China University of Technology, Guangzhou, 510640, China

6 Key Laboratory of Ocean Energy Utilization and Energy Conservation of Ministry of Education, Dalian University of Technology, Dalian, Liaoning 116024, China

ABSTRACT

Gas hydrate is an ideal alternative energy source with high energy density and low combustion pollution. Based on the different distribution of methane hydrate, free gas and free water, gas hydrate deposits can be classified into four classes (Class 1, 2, 3 and 4). TOUGH+HYDRATE was used to simulate the dissociation process of depressurization in gas and water excess Class 2 and 3 methane hydrate deposits. The initial state and production pressure selection were the same as the experimental results. The simulation results were compared with the experimental results. In water excess condition, gas production volume in simulation is 1/3 higher than that in experiment, except hydrate production under 2.0 and 2.3 MPa in Class 3 deposit. It was found that the minimum temperature in simulation is larger than that in experiment during depressurization in Class 2 and 3 methane hydrate deposits when gas is excess.

Keywords: methane hydrate, depressurization, water excess, gas excess

1. INTRODUCTION

As a new type of potential fossil fuel resource, natural gas hydrates have been widely investigated in

recent years[1, 2], with the final goal of recovering natural gas safely and efficiently[3-5]. At present, it's considered that there are four classes natural gas hydrate deposits (Class 1, 2, 3 and 4)[6]. The distribution difference of methane hydrate, free gas and free water in these four types of deposits results in different production rate and temperature properties during exploitation. A variety of techniques have been applied in laboratory studies of gas hydrate production experiments in order to quantify the gas production rate, spatial distributions of in-situ phase saturations and P-T properties[7-9]. However, experimental researches mainly focus on Class 1, 2, 3 deposit. As no upper and lower impermeable layer exist in Class 4 deposit and hydrate saturation is low, this type of deposit is not considered as a mining target. Researches on these four classes of gas hydrate deposit exploitation is mostly limited to simulation. Although hydrate formation and dissociation properties by experiment and simulation methods have been compared by Zhang *et al.*[10, 11], hydrate production in different types of hydrate deposits need further interpreted.

These authors contributed equally to this work.

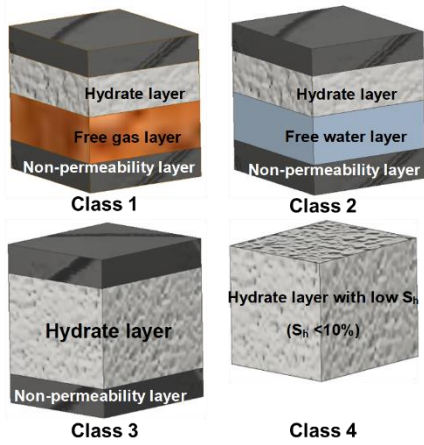


Fig.1 Four types of hydrate deposits[6]

2. RESEARCH METHODS

2.1 Experiment method

Experimental system and method were described in previous article and experimental system is shown in Fig.2 [12].

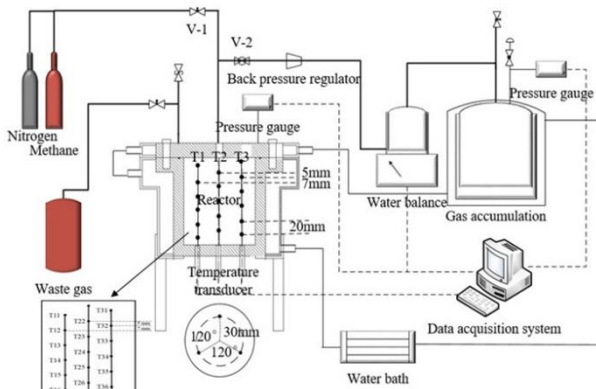


Fig. 2 Experimental system for hydrate formation and dissociation

2.2 Simulation method

The simulations in this study were conducted by the T+H code[13], a numerical simulator developed at the Lawrence Berkeley National Laboratory (LBNL) to model the non-isothermal behavior of methane production, phase change and flow. It can simulate conditions where typical of methane hydrate deposits by solving the coupled equations of fluids and heat balance associated with such systems. MeshMaker application[13] was used to construct the grid of the 2D axisymmetric cylindrical simulation domain, which is shown in Fig.3. That represents the accurate geometry of the high-pressure reactor shown in Fig. 2. A very fine spatial discretization was used for maximum accuracy. The interior of the

reactor with a radius $r=51.5$ mm was discretized into 26 subdivisions ($1 \times \Delta r=1.5$ mm and $25 \times \Delta r=2.0$ mm), and the reactor wall thickness ($d_{wall}=6.0$ mm) was discretized into 2 subdivisions ($2 \times \Delta r=3.0$ mm) in order to accurately capture heat transport between the interior of the reactor and the circulating. The internal height of the reactor is 120 mm, which was discretized into 48 subdivisions ($48 \times \Delta z=0.25$ mm). The top and bottom is 15 mm ($3 \times \Delta z=0.5$ mm). The whole reactor was discretized into $29 \times 54=1566$ subdivisions.

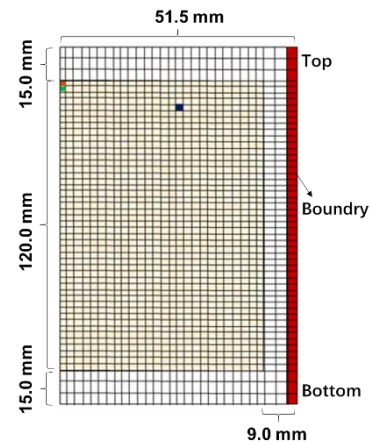


Fig. 3 Schematic of the mesh of the simulation domain

3. RESULTS AND DISCUSSION

3.1 Gas production properties in experiment and simulation

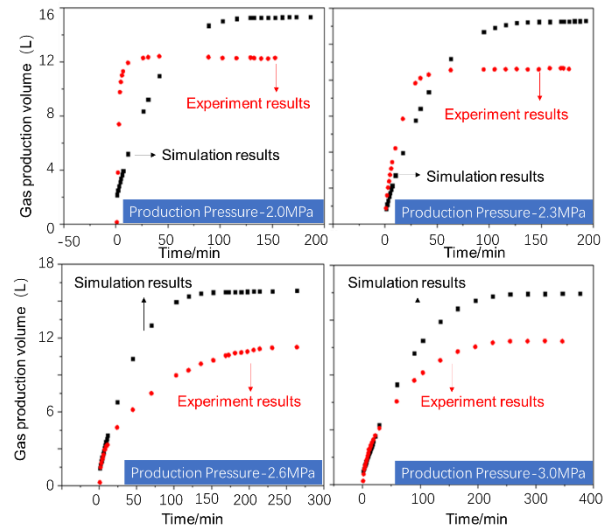


Fig. 4 Gas production in Class 2 deposit with water excess

Gas production properties in Class 2 deposit with water excess is shown in Fig.4. Hydrate dissociate under a range of production pressure :2.0 MPa, 2.3MPa,2.6

MPa and 3.0 MPa in this study. As shown in Fig. 4, simulation gas production volume is higher than experimental results. Simulation results curves have similar shape under different production pressure in Fig.4. That means hydrate dissociate continuously but production pressure has effect on hydrate dissociation ending time. The ending time gets longer with production time increasing, which is similar in experiment. When production pressure becomes higher, hydrate dissociation driving force get smaller and then hydrate dissociate slower. Under 2.0 and 2.3 Mpa, gas products faster in experiment than simulation, which is contrary under 2.6 MPa and 3.0 MPa.

Comparison of the simulation and experiment result about gas production in Class 3 deposit with water excess is shown in Fig.5. The same rules were found in Class 3 deposit with Class 2. Experimental gas production volume are higher than simulation result under 2.0 MPa and 2.3 MPa. However, the experimental and simulation results are much closer in Class 3 deposit under 2.0 MPa and 2.3 MPa. In Class 2 and Class 3 deposit, gas production rate has the same rules. Under 2.0 and 2.3 MPa, experiment gas products faster at the initial time. When the production pressure increases to 2.6 and 3.0 MPa, gas products faster in simulation form initial time.

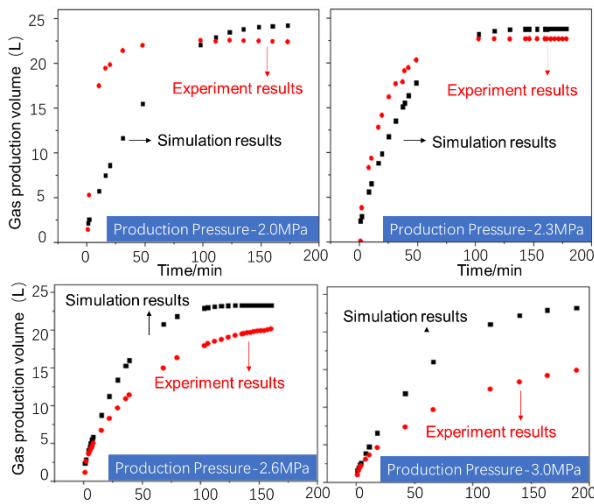


Fig.5 Gas production in Class 3 deposit with water excess

3.2 Temperature properties

Temperature changes during hydrate production in simulation and experiment is shown in Fig.6. Temperature changes are seriously different between experiment and simulation. In experiment when methane hydrate dissociated for about 30 min, the temperature researches to the lowest point which is -

1.7 °C, but the lowest temperature just drops to 0.5 °C in simulation. That could be caused by several reasons. First, the expression of TOUGH+HYDRATE Joule-Thomson effect maybe not accurate, or the temperature changes caused by gas expansion is different due to the different gas flow in the process of experiment and simulation. Second, the initial condition is above hydrate equilibrium curve in simulation. When the simulation starts, the condition at this time could cause hydrate formation before original hydrate dissociate. Hence, at the initial period of dissociation, decomposed hydrate is less than formed hydrate, which break the balance of heart. That means formed hydrate is more than decomposed hydrate. Then released heat from hydrate formation makes temperature much higher.

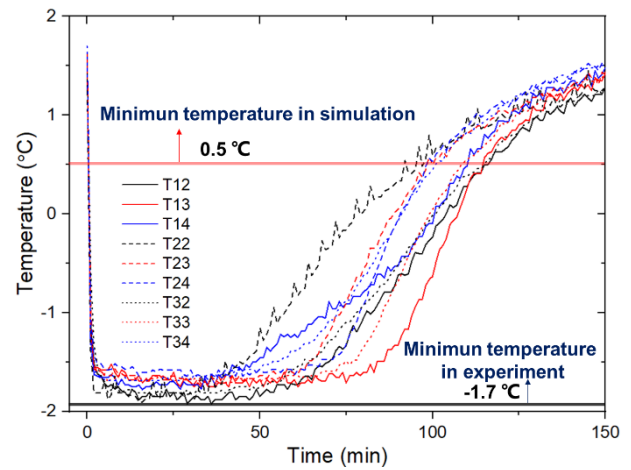


Fig.6 Temperature changes when methane hydrate dissociates under 2.3 MPa in Class 2 deposit with gas excess

The methane hydrate saturation, temperature, water saturation and methane saturation distribution of gas-excess Class 2 deposits under 2.3 MPa production pressure is shown in Fig.7. Hydrate didn't dissociate before 120 min, but due to the free gas release, the temperature of methane hydrate region started to decrease. In methane hydrate region, the temperature increases radially from the central position to the edge. The reason for this phenomenon is that the free gas release causes the Joule-Thomson effect, resulting in the decrease of temperature. However, there is no heat source in the hydrate reservoir, and the surrounding environment transfers heat inward. Temperature distribution has relationship with hydrate saturation, water saturation and gas saturation.

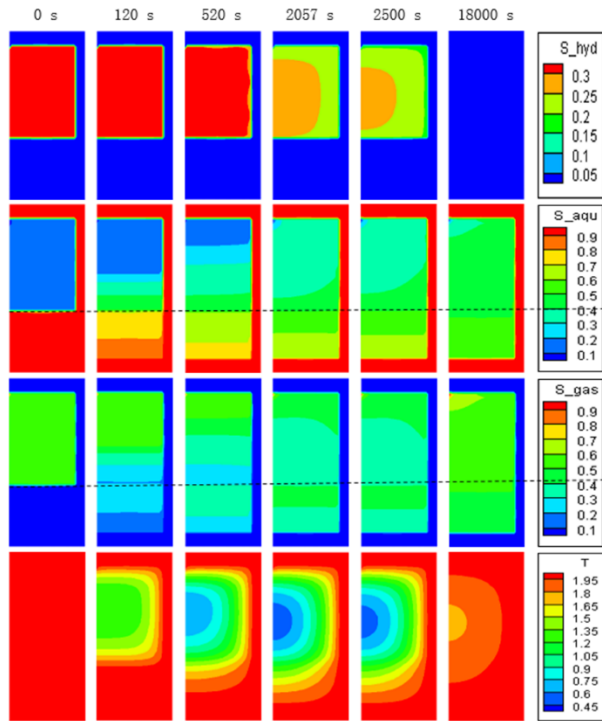


Fig.7 The methane hydrate saturation, temperature, water saturation and methane saturation distribution of gas-excess Class 2 deposits under 2.3 MPa backpressure

4. CONCLUSION

Experiment and simulation results about hydrate production in Class 2 and Class 3 deposit were compared in this study. In water excess condition, gas production volume in simulation is 1/3 higher than that in experiment except hydrate production under 2.0 and 2.3 MPa in Class 3 deposit. It was found that the minimum temperature in simulation is larger than that in experiment during depressurization in Class 2 and 3 methane hydrate deposits when gas is excess. Multi-phase distribution should be further studied by experiment and simulation.

ACKNOWLEDGEMENT

This project was financially supported by the China Postdoctoral Science Foundation (2019TQ0302), Natural Science Foundation of China (41873069), China Postdoctoral Science Foundation (2019M652891) and the National Natural Science Foundation of China (51436003).

REFERENCE

[1] Z.R. Chong, S.H.B. Yang, P. Babu, P. Linga, X.-S. Li, Review of natural gas hydrates as an energy resource:

Prospects and challenges, *Applied energy*, 162 (2016) 1633-1652.

[2] E.D. Sloan Jr, C.A. Koh, *Clathrate hydrates of natural gases*, CRC press 2007.

[3] Q. Yuan, C.-Y. Sun, X. Yang, P.-C. Ma, Z.-W. Ma, Q.-P. Li, G.-J. Chen, Gas production from methane-hydrate-bearing sands by ethylene glycol injection using a three-dimensional reactor, *Energy & Fuels*, 25 (2011) 3108-3115.

[4] G. Li, X.-S. Li, B. Yang, L.-P. Duan, N.-S. Huang, Y. Zhang, L.-G. Tang, The use of dual horizontal wells in gas production from hydrate accumulations, *Applied energy*, 112 (2013) 1303-1310.

[5] J.-C. Feng, Y. Wang, X.-S. Li, Z.-Y. Chen, G. Li, Y. Zhang, Investigation into optimization condition of thermal stimulation for hydrate dissociation in the sandy reservoir, *Applied energy*, 154 (2015) 995-1003.

[6] G. Moridis, Numerical studies of gas production from Class 2 and Class 3 hydrate accumulations at the Mallik Site, Mackenzie Delta, Canada, *SPE Reservoir Evaluation & Engineering*, 7 (2004) 175-183.

[7] S. Wang, M. Yang, P. Wang, Y. Zhao, Y. Song, In situ observation of methane hydrate dissociation under different backpressures, *Energy & Fuels*, 29 (2015) 3251-3256.

[8] L. Yang, Y. Liu, H. Zhang, B. Xiao, X. Guo, R. Wei, L. Xu, L. Sun, B. Yu, S.J.C.J.o.C.E. Leng, The status of exploitation techniques of natural gas hydrate, (2019).

[9] L. Yang, L. Ai, K. Xue, Z. Ling, Y.J.E. Li, Analyzing the effects of inhomogeneity on the permeability of porous media containing methane hydrates through pore network models combined with CT observation, 163 (2018) 27-37.

[10] Z. Yin, G. Moridis, Z.R. Chong, H.K. Tan, P. Linga, Numerical analysis of experiments on thermally induced dissociation of methane hydrates in porous media, *Industrial & Engineering Chemistry Research*, 57 (2017) 5776-5791.

[11] Z.R. Chong, G.A. Pujar, M. Yang, P. Linga, Methane hydrate formation in excess water simulating marine locations and the impact of thermal stimulation on energy recovery, *Applied energy*, 177 (2016) 409-421.

[12] Y. Gao, M. Yang, J.-n. Zheng, B. Chen, Production characteristics of two class water-excess methane hydrate deposits during depressurization, *Fuel*, 232 (2018) 99-107.

[13] G. Moridis, User's Manual of the TOUGH+ Core Code v1. 5: A General-Purpose Simulator of Non-Isothermal Flow and Transport through Porous and Fractured Media, (2014).